Sensors & Transducers, Vol. 178, Issue 9, September 2014, pp. 244-249

Sensors & Transducers

Extremum Search Based Welding Defect Inspecting Algorithm of X-ray Digital Sensor

[1,2] Wei LIANG, [3] Liang TAO and [1] Guangxian ZHANG

[1] Department of Control Science and Engineering Shandong University, Jing 10 Road, Jinan, Shandong, 250061, China
[2] Jinan Engineering Vocational Technical College, Jinan 250200, China
[3] School of Information and Electrical Engineering, Shandong Jianzhu University, Jinan 250101, China
[1] Tel.: +86 15966677299
[1] E-mail: dzhlw0918@sohu.com

Received: 11 April 2014 /Accepted: 29 August 2014 /Published: 30 September 2014

Abstract: This paper briefly presents an inspecting algorithm of welding defect location based on grayscale value distribution curve. It is used to locate the welding line position and the defects. Firstly, the amorphous silicon detector based system acquires original digital images. The noise was suppressed by average time field method. Furthermore, the aliasing between the defects and the noise was decreased. The grayscale value summation was adopted to extract the welding line. The attenuation law demonstrated that the transmitted X-ray intensity is directly proportional to the input intensity and inversely proportional to the workpiece thickness. It adopts the curve of line gray value of weld to discover the location of welding defect. The experimental result proved high accuracy and efficiency. *Copyright © 2014 IFSA Publishing, S. L.*

Keywords: X-ray digital imaging, Welding line, Defect detection, Image processing.

1. Introduction

Detecting the defects like the stomas, slag inclusion and lack of penetration is the important link evaluating the welding technology and its detection precision directly influences the judgment to the qualification or disqualification of welded piece. At present, there are many methods to detect the weld defects, such as the destructive detecting method, infrared ray, ultrasonic wave and X-ray. X-ray is widely used in the non-destructive detecting field for its good instantaneity and high precision coefficient digitization [1, 2]. Comparing with the traditional film ray detecting method's shortcomings that the time is long and the process is complex, and the automatic online detection can't be realized and the dependency on the human is strong, etc. The digital X-ray detecting speed is fast, and the operation is easy and can realize the real time digital imaging, which is to the benefit of image later-period strengthening and disposing. This paper researches the extraction to the weld defect position by the amorphous silicon digital detector.

2. Imaging Principle

X-ray digital imaging system is composed of X-ray source, FPD (Flat Panel Detector), the corresponding control equipment and workpiece model is shown in Fig. 1.

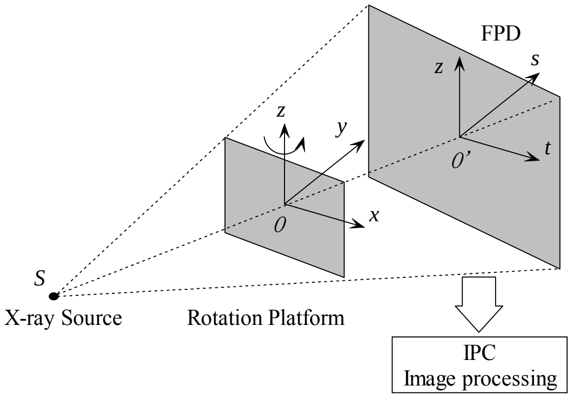

Fig. 1. System model.

The X-ray source generates X-ray. The X-ray transmits through the workpiece and projects on the FPD. At last, the digitalized images are transmitted to the IPC (Industrial Personal Computer) for further processing.

The adopted FPD in this paper is an amorphous silicon digital detector named Paxscan2520. Its sensitive element receiving the X-ray is a thin scintillating medium screen, which can transfer the photon to the visible light, and the said visible light will be transferred to the digital image by the large-scale integration amorphous silicon photodiode array, as shown in Fig. 2 [3, 4]. The pixel size of Paxscan2520 is 127 μm^2. The grayscale level is 12 bit. The digital FPD can collect the high quality digital images in a high speed. The image dynamic range is large and the signal-to-noise ratio is high.

The X-ray source adopts GECCO2505 portable X-ray machine with the tube voltage 110~250 kV, tube current 2 mA, focus size 2 mm × 2 mm and maximum 46 mm penetrating thickness (A3 steel), as shown in Fig. 3.

Fig. 2. Flat panel detector.

Fig. 3. Gecco2505 X-ray machine.

3. Welding Line Segmentation Algorithm

3.1. Image Noise Reduction

The noise is the most important factor influencing X-ray detecting quality. The noise of the digital image must be reduced firstly to acquire proper welding line.

The imaging system noise is from the followings: Firstly, X-ray photon fluctuation noise. The mathematical distribution complies with poisson distribution. For example, if there are $\sqrt{N}$ photons' natural fluctuation in N photons. Secondly, dark current noise, KTC noise (reset noise), quantizing noise and readout noise. The dark current noise is from the electron thermal motion, which is relevant to the temperature, so we can restrain that effectively through the refrigeration technique; KTC noise can be restrained through the rational circuit design; the quantizing noise is relevant to the digitalizing bit, which is that the larger the bit is, the smaller the quantizing noise will be; the readout noise is relevant to the readout speed, which is that the higher the readout speed is, the larger the readout noise will be [2, 5].

This paper adopts the time sequence frame to superpose the average and median filtering to jointly reduce the noise. We take the time sequence frame to remove the random noise by filtering through superposition and remove the impulse noise with median filtering.

The so-called frame averaging in the time sequence is that conducting the average calculating operation of inter-frame corresponding point grey level to the obtained a series of images under the condition of identical transillumination and different time sequences, and getting a image D [6]. The algorithm is shown in equation (1)

$$D(i, j) = \frac{1}{m}\sum_{i=1}^{h}\sum_{j=1}^{w}\sum_{t=1}^{m} F_t(i, j), \qquad (1)$$

where $F_t(i, j)$ is the sequence image at time t, i and j are the coordinate values of the image pixel, h and w are image height and width respectively, m is the superposed frame number.

If we use the Paxscan2520 flat panel detector and when we set the penetrating tube voltage as 140 kV, and the tube current as 2 mA, and the focal length as 70 cm, and the frame period as 5.5 fps, and make the m=1, 4, 8, 16, 32, 64 and 128. The measured data is shown in Table 1. Then we get 7 times sequence average calculating operation images, and the superposed frame number and noise quantity coordinate relationship is shown in Fig. 4.

Table 1. Measured noise amount.

Frames	1	4	8	16	32	64	128
Noise	8.54	3.55	2.83	2.53	1.77	1.43	1.41

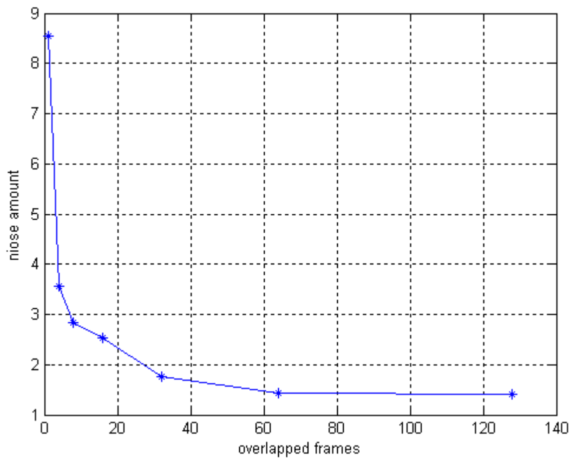

Fig. 4. The residual noises of image integral.

From Fig. 4, we can know that the noise quantity basically tends to gentle after 32 image additions, i.e. the random noise fundamentally gets the stable restraint.

After the time sequence frame superposing average filter, we shall establish an odd number movable platen and make the mid-value of each point in the template to replace the central point value. From the principle, we can know that if we want to make the median filtering to one image, we must firstly sort the wanted pixels in the template and its neighboring region's pixel value, and define the mid-value, and then give that mid-value to this pixel. The image after the median filtering is to make the pixel with different gray levels seem to close to its adjacent value.

If we set the raw image as $A(i, j)$, and window size as $(2k+1)*(2k+1)$, then the image $G(i, j)$ after the mid-value disposing can be as [7, 8].

$$G(i, j) = \operatorname*{med}_{s=-k}^{k}{}_i \operatorname*{med}_{t=-l}^{l}{}_j [A(i+s, j+t)], \tag{2}$$

After the 32 frames superposition averaging and 3*3 median filtering, the noise signal influence reduces.

To reduce the total calculated quantity of the image disposing, and at the same time, avoid the unnecessary false detection at the welded joint, we shall extract the welded joint region before realizing the defect extraction [9].

3.2. Welded Joint Region Extraction

We get the welded joint region with the grey level and waveform analysis method and extract the welded joint region through summarizing the grey level of the rank which is parallel to the welded joint direction in the raw image in the Fig. 5(a). The steps are as follows:

Step 1: Summarize the rank pixel in image $A(x, y)$ as $D(x) = \sum A(x)$. After the summarization, the grey level and variation tendency are in Fig. 5(b).

Step 2: Calculate the second order difference $D''(x)$ to gray level and $D(x)$, and find out the gray level summarization second order difference distribution regularity, which are in Fig. 5(c), and we can search out the minimal value point K, and search the two maximum values K_1 and K_2 near the minimal value to define the boundary of the welded joint, and in Fig. 5(c), the red region marked values are the minimal value and its two surrounding maximum values.

Step 3: Extract the center section between K_1 and K_2, i.e. $[K_2, K_3]$ is the welded joint region, which is in Fig. 5(d).

4. Defect Detection

4.1. Welding Line Image Equalization

To detect the defect correctly, we need to equalize the welded joint image. The histogram equalization can be used to adjust the image with uneven gray level distribution to realize the strengthening. After the equalizing to the raw image, the result shows that when we reach the 32 level equalization, the image brightness value frequency tends to the smooth and steady condition, which effectively strengthens the dynamic range and contrast ratio. Fig. 6 is the effect after taking the histogram equalization, and after that histogram equalization, the dynamic range of detail point has been improved and the welded joint has been clearer.

4.2. Defect Detecting Algorithm

Based on the ray attenuation law, when the ray passing through a substance, if the passing distance l changes as $\mathrm{d}l$, then the substance satisfies the followings to the ray intensity I attenuation.

$$\mathrm{d}I = -\mu(E) I \mathrm{d}l, \tag{3}$$

From the formula (3), we can know that the intensity decrement dI is in direct proportion to the entering ray intensity and passed substance thickness l. The density of the general welded additional metal (like the welding rod) and parent metal density are basically the same, so under the defect-free condition, the gray level distribution and thickness proportion relationship is in formula (4),

$$I(E) = I_0(E) * e^{-\mu(E)l}, \tag{4}$$

where I0 is the entering ray intensity without absorber, I is the penetrating ray intensity, μ is the substance attenuation coefficient.

For that the radial absorptivity seriously relies on the material density, and if there are defects (like the slag inclusion or pore) in the even material, then the different ray intensities of the ray passing through the workpiece's different parts will make the defects detected out [10-15].

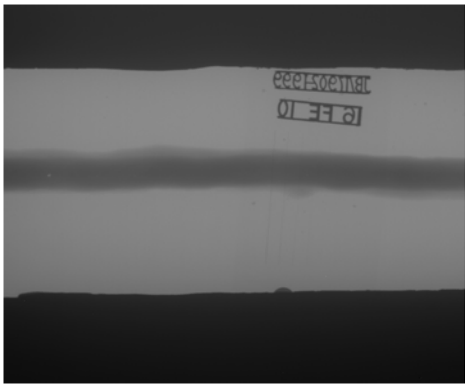

(a) Original image

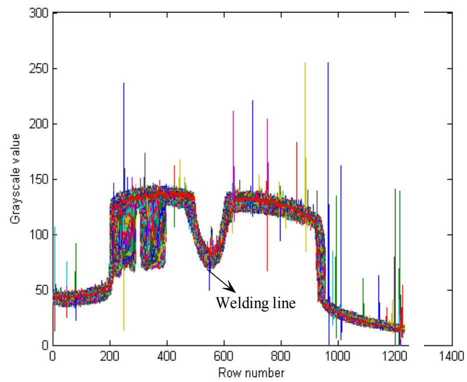

(b) Pixel grayscale trend

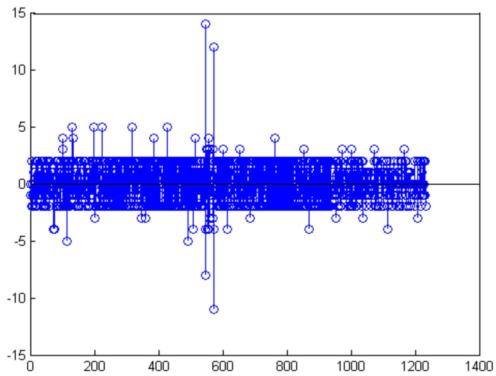

(c) two order derivative distribution

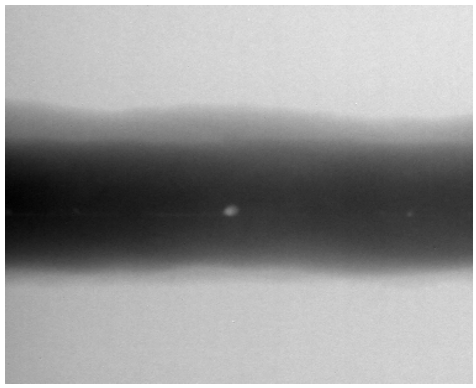

(d) Recognized welding line

Fig. 5. Process of weld extraction.

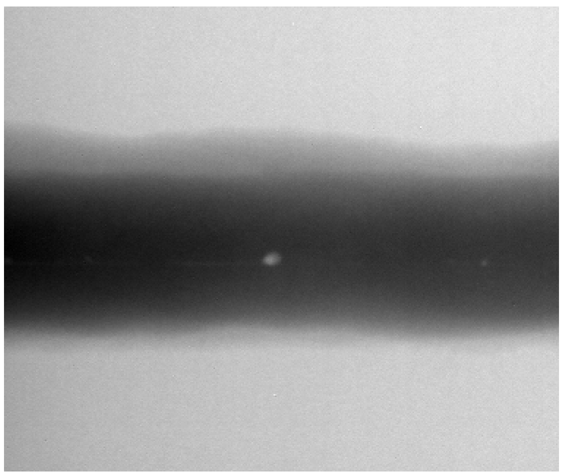

Fig. 6. Welding line image after histogram equalization.

At one rank which is perpendicular to the welded joint but doesn't pass through the defect, the rank grey level approximately is in bell-shaped distribution, i.e. grey level distribution of rank which doesn't pass through the welded joint defect is in unimodal condition; when the rank which is perpendicular to the welded joint and passes through the defect, the rank grey level distribution has trench or the rising slope changes, i.e. the grey level of rank which passes through the welded joint is in double-peak wave shape. The raw image of the welded joint is shown in Fig. 7(a), and the unimodal and double-peak wave is shown in Fig. 7(b).

From Fig. 7, we know that when one rank which is perpendicular to the welded joint but doesn't pass through the defect, the rank grey level approximately is in bell-shaped distribution, i.e. grey level distribution of rank which doesn't pass through the welded joint defect is in unimodal condition; when the rank which is perpendicular to the welded joint and passes through the defect, the rank grey level distribution has trench or the rising slope changes, i.e. the grey level of rank which passes through the welded joint is in double-peak wave shape. Then we can analyze that from that wave, and define the position of the welded joint and find out the position of the defect, after that, we can define the defect boundary and analyze the defect type.

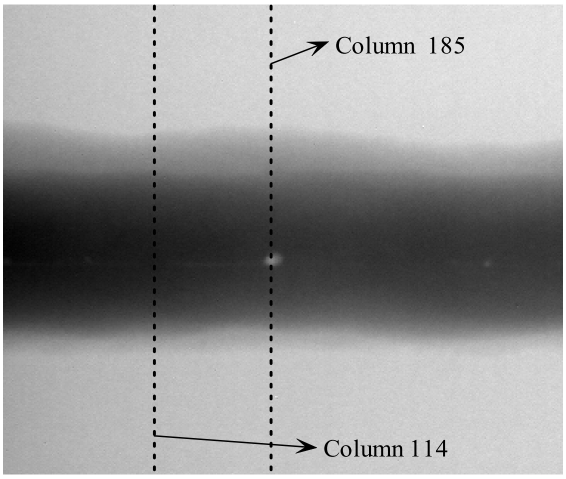

(a) Original welding line image

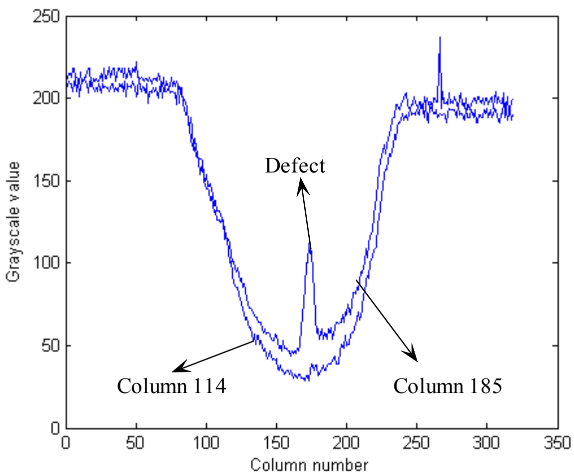

(b) Single and double peaks waveform

Fig. 7. Gray scale distribution.

4. Conclusion

The algorithm proposed by this paper effectively restrains the noise and enhances the details. Furthermore, it located the welding line and distracts the defects efficiently. The algorithm has the advantages of high detection precision and low complexity.

Acknowledgements

This work is supported by Shandong provincial outstanding young scientist award fund project (BS2013DX045), Shandong provincial high school development project (J13LG52), Shandong provincial high school development project (J11LG16), national natural science foundation of China (51207083), Shandong provincial outstanding young scientist award fund project (BS2013DX018), science and technology project of MOHURD (2011-K1-55), Shandong Jianzhu university doctoral fund project (XNBS1249).

References

[1]. Gao Yan, Kong Fan-Qin, Inspection of weld imperfection base on the digital radiography, *Welding Technology*, Vol. 32, Issue 2, 2003, pp. 13-14.

[2]. Kong Fan-Qin, Lu Hong-Nian, Welding quality inspection by digital radiography, *Nondestructive Testing*, Vol. 30, Issue 1, 2008, pp. 20-22.

[3]. Liang Li-Hong, Kong Fan-Qin, Lu Hong-Nian, The analysis of level B imaging quality based on the X-ray flat-panel detector, *Nondestructive Testing*, Vol. 27, Issue 3, 2005, pp. 113-116.

[4]. Huang Kui-Dong, Zhang Ding-Hua, Li Ming-Jun, Scatter detection and correction method of FPD-based DR/CT imaging systems, in *Proceedings of the Conference on Electronic Measurement & Instruments*, Beijing, 2009, pp. 102-105.

[5]. Ma Yue-Zhou, Ai Wei-Ping, Zhang Chang-Qing, X-ray digital imaging quality of flat panel detector, *Journal of Lanzhou University of Technology*, Vol. 33, Issue 2, 2007, pp. 20-24.

[6]. Wang Bao-Ping, Fan Jiu-Lun, Xie Wei-Xin, et al, Histogram based adaptive filter for removing image noise, *Acta Electronica Sinica*, Vol. 32, Issue 7, 2004, pp. 1176-1179.

[7]. Hou Run-Shi, Shao Jia-Xin, Wang Li, et al, Image processing of real-time automatic X-ray inspection system for weld defects, *Nondestructive Testing*, Vol. 31, Issue 2, 2009, pp. 99-102.

[8]. Huang Kui-Dong, Zhang Ding-Hua, Li Ming-Jun, Scatter detection and correction method of FPD-based DR/CT imaging systems, in *Proceedings of the Conference on Electronic Measurement & Instruments*, Beijing, 2009, pp. 16-19.

[9]. Shao Jia-Xin, Du Dong, Zhu Xin-Jie, et al, Weld defect detection of double sides weld based on X-ray digitized image, *Welding Journal*, Vol. 31, Issue 11, 2010, pp. 21-24.

[10]. Zhang Xiao-Guang, Gao Ding, The X-ray testing welding defects extraction and automatic identification, *National Defense Industry Press*, 2004.

[11]. Zuo Kai, Sun Tong-Jing, Li Zhen-Hua, Compton scattering based method of objects thickness, *Journal of Shandong University: Engineering Science*, Vol. 39, Issue 6, 2009, pp. 68-72.

[12]. Tao Liang, Sun Tong-Jing, Li Zhen-Hua, et al, Neighborhood contrast based adaptive enhancement of X-ray digital image, *Nondestructive Testing*, Vol. 33, Issue 1, 2011, pp. 20-22.

[13]. Kong Fan-Qin, Chao Jia-Qiang, Zhang Guang-Xian, et al, New digital radiography technology of welding quality, *Electric Welding Machine*, Vol. 36, Issue 10, 2006, pp. 29-31.

[14]. Tao Liang, Sun Tong-Jing, Li Zhen-Hua, et al, Diffraction and transmission optical model based edge location algorithm, *Journal of Shandong University: Engineering Science*, Vol. 42, Issue 4, 2012, pp. 54-59.

[15]. J. Britten, Zhechuan Feng, Gu Xu, Magnified hard X-ray image in one dimension, *Applied Physics Letters*, Vol. 96, Issue 26, 2010, pp. 261907-261907-3.
